Journal of the Korean Ceramic Society
Vol. 54, No. 5, pp. 366~379, 2017.

https://doi.org/10.4191/kcers.2017.54.5.12

Review

Electrospun Metal Oxide Composite Nanofibers Gas Sensors: A Review

Zain Ul Abideen*, Jae-Hun Kim*, Jae-Hyoung Lee*, Jin-Young Kim*, Ali Mirzaei, Hyoun Woo Kim**,***,†, and Sang Sub Kim*,‡**

**Department of Materials Science and Engineering, Inha University, Incheon 22212, Korea*
***The Research Institute of Industrial Science, Hanyang University, Seoul 04763, Korea*
****Division of Materials Science and Engineering, Hanyang University, Seoul 04763, Korea*

(Received August 18, 2017; Accepted September 11, 2017)

ABSTRACT

Nanostructured materials have attracted considerable research interest over the recent decades because of their potential applications in nanoengineering and nanotechnology. On the other hand, the developments in nanotechnology are strongly dependent on the availability of new materials with novel and engineered morphologies. Among the novel nanomaterials reported thus far, composite nanofibers (NFs) have attracted considerable attention in recent years. In particular, metal oxide NFs have great potential for the development of gas sensors. Highly sensitive and selective gas sensors can be developed by using composite NFs owing to their large surface area and abundance of grain boundaries. In composite NFs, gas sensing properties can be enhanced greatly by tailoring the conduction channel and surface properties by compositional modifications using the synergistic effects of different materials and forming heterointerfaces. This review focuses on the gas sensing properties of composite NFs synthesized by an electrospinning (ES) method. The synthesis of the composite NFs by the ES method and the sensing mechanisms involved in different types of composite NFs are presented along with the future perspectives of composite NFs.

Key words : Nanofiber, Metal oxide, Electrospinning, Sensing mechanism, Gas sensor

1. Scope of the review

This paper introduces metal oxide-based gas sensors, the synthesis of metal oxide composite NFs by electrospinning (ES), and the sensing mechanism involved in composite NFs gas sensors. Despite the many reviews and books on gas sensors,[1-5] this paper focuses only on the developments of metal oxide composite NFs for gas sensing applications, on which no review has been published. Owing to the broad scope of the topic, other one-dimensional nanostructures and NFs synthesized by the methods other than ES are not included. Accordingly, this review is confined to electrospun metal oxide composite NFs synthesized by ES along with their gas sensing mechanisms.

2. Metal Oxide-Based Gas Sensors: An Introduction

By definition,[6] an air pollutant is any substance that can have detrimental effects on humans, animals, vegetation, or even materials. Regarding humans, air pollution can cause or contribute to an increase in mortality or serious illness. According to Kampa *et al.*,[6] air pollutants can be grouped into four categories (i) gaseous pollutants (e.g. NO_x, SOx, CO, O_3, and volatile organic compounds (VOCs)); (ii) persistent organic pollutants, such as dioxins; (iii) heavy metals, such as Pb and Hg; and (iv) particulate matter. Among these pollutants, toxic gases emitted mainly from the combustion of fossil fuels are the most important contributors to air pollution, and air pollution due to the presence of toxic gases is currently one of the main issues associated with modern life, particularly in big cities. Although the human nose is an extremely advanced sensor that is capable of detecting and distinguishing hundreds of different gases instantly, it fails if the gas concentration is very low or the gas is odorless, such as CO or H_2.

Accordingly, there is a huge demand for devices that support the human nose, namely gas sensors.[7] Gas sensors are a subgroup of chemical sensors and by definition, a chemical gas sensor is a device, which upon exposure to a gas molecule, changes one or more of its physical properties in a way that can be measured and quantified.[8,9] Gas sensors are currently used extensively in houses, factories, laboratories, hospitals, and almost all technical installations.[10] Today, the most common gas sensors are surface acoustic waves gas sensors,[11] optical gas sensors,[12] catalytic gas sensors,[13] electrochemical gas sensors,[14] microwave gas sensors,[15] and metal oxide-based gas sensors.[16]

Metal oxide-based gas sensors are the most widely used type of gas sensor owing to their strong response, high stability, and low cost.[10,17] Their history dates back to 1952,

†Corresponding author : Hyoun Woo Kim
E-mail : hyounwoo@hanyang.ac.kr
Tel : +82-32-860-7546 Fax : +82-32-862-5546
‡Corresponding author : Sang Sub Kim
E-mail : sangsub@inha.ac.kr
Tel : +82-32-860-7546 Fax : +82-32-862-5546

when Brattain and Bardin discovered that the resistance of Ge changes upon exposure to different gases.[18-21] Shortly after this great discovery, Seiyama *et al.*,[22,23] demonstrated these effects in ZnO, and Taguchi *et al.*[24,25] introduced the first metal oxide-based gas sensors in Japan. Currently, SnO_2 and ZnO are the most widely studied metal oxides for gas sensing applications because of their high sensitivity to different gases along with high stability.[26] Nevertheless, the main problem associated with these metal oxides and most metal oxides is their poor selectivity.[1] Therefore, many strategies have been proposed to enhance the selectivity and sensing performance of gas sensors.[27-29] The most common approaches include the use of nanomaterials with high surface areas;[30,31] addition of dopants, such as Fe,[32] Co,[33] and Cu (dispersed as ions in the oxide structure);[34] functionalization with noble metals, such as Ag, Au, Pt, and Pd;[35,36] modification of the electric properties of the metal oxides either by electronic sensitization[37,38] or by a spillover effect;[39,40] and formation of heterostructures using composite materials.[41-45]

Although the aforementioned techniques are effective for achieving selectivity in metal oxide-based gas sensors,[27,46,47] the sensitivity and selectivity of metal-oxide gas sensors by these methods are insufficient for all applications, particularly when the interfering gases have similar compositions or the gas concentration is in the sub-ppm level. Accordingly, a combination of these approaches is used for the fabrication of high performance gas sensors. One efficient combined approach is the fabrication of composite NFs for sensing applications.

3. Nanofibers (NFs)

As the primary factor for gas sensors is a large surface area, nano materials with high surface areas have superior advantages for improving the sensing performances of gas sensors over their bulk counterparts.[48,49] The morphological engineering of nanomaterials in recent years has led to the introduction of one-dimensional (1D) nanostructures, such as nanowires,[50] nanobelts,[51] nanotubes,[52] nanorods,[53] and NFs,[54] which have several unique advantages, such as large surface-to-volume ratio, small dimensions comparable to the Debye length, superior stability, and ease of fabrication and functionalization.[55-57] Furthermore, they can be integrated with a field-effect transistor (FET) configuration that allows the use of a gate potential controlling the sensitivity and selectivity.[57,58] On the other hand, NFs among 1D nanostructures, have been identified as the most promising structures for gas sensing applications. They have higher surface-to-volume ratios than other 1D nanostructures due to the presence of a large number of nanograins and a web like configuration. Therefore, their surfaces are readily exposed to gas molecules, resulting in high sensitivity and rapid response.[59]

4. Synthesis of Electrospun Composite NFs

Although there are other techniques for the synthesis of NFs, such as solution/melt blowing,[60] sol-gel templating,[61] centrifugal spinning,[62] and self-assembly,[63] most of the composite metal oxide NFs for gas sensing applications are synthesized by the ES method. This can be traced back to 1934 when Formhals *et al.* invented an experimental set-up for producing polymer filaments.[64] Since the 1990s, ES has been studied extensively.[65] ES is the simplest and most versatile technique to generate a range of structures with different configurations, such as normal, aligned, hollow, porous and core-shell of 1D nanostructures from various materials, even from ceramics.[66] This method is a highly flexible technique for producing long and continuous NFs using solutions,[67,68] gels and liquid crystals,[69] melts[70] and emulsions.[71-73] Moreover, with the increasing number of ES companies in recent years, ES is expected to move progressively from a laboratory bench process to an industrial scale process.[74] From a commercial point of view, ES is the only method of choice for the large scale preparation of NFs compared to other available methods, due to the easy handling, minimum consumption of solution, controllable NF diameter, low cost, simple, and reproducible nature in processing NFs as well as technical advances over other methods (scale up process).[75] Accordingly, composite metal oxides can be produced easily and massively on a commercial scale by a straightforward, very low cost, versatile, and facile ES process. This review explains the fundamentals and basic set-up of the ES process to synthesize the composite metal oxide NFs for gas sensing applications. The reader can refer to the other published papers for more information on the ES method.[65,73,76-79]

ES involves the uniaxial stretching of a viscoelastic polymeric or melt solution based on electrostatic interactions. Fig. 1(a) presents the ES set-up, which basically consists of three components: a high voltage power supply (mostly DC but AC is also feasible,[80,81] a spinneret (a metallic needle), and a collector that is electrically conductive. The needle is

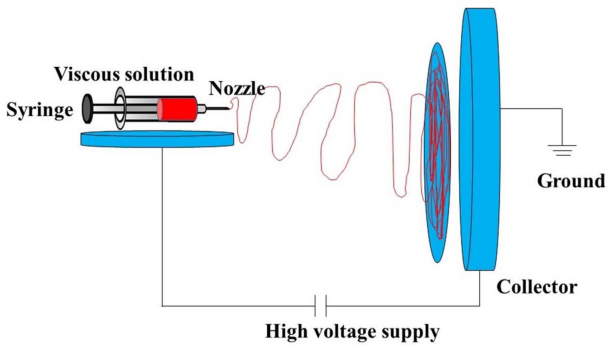

Fig. 1. Schematic illustration of the ES process for the production of NFs.

attached to a plastic syringe that is loaded with the precursor/polymer solution. Because the quality and final properties of NFs depends greatly on the quality and size of the needle, the syringe is mostly connected to a syringe pump that can maintain a constant feeding rate of the solution through the spinneret. The collector is usually an aluminum foil to collect the NFs but it can be of any material and in any configuration according to the required end product. The collector is positioned at a certain distance from the needle. This setup is usually enclosed in a box so that the atmosphere (humidity) can be controlled and varied according to the requirements. Under an applied high voltage (usually 1 - 30 KV), the drop at the needle tip deforms into a conical shape, known as a Taylor cone, due to the presence of two major electrostatic forces: electrostatic repulsion between the surface charges, and Coulombic forces exerted by the external electric field. After a certain threshold value, the applied electric field overcomes the surface tension of the solution and ejects the drop from the needle towards the collector in the form of a long and thin thread. The diameter of the jet decreases as it reaches the ground target where the NFs are collected. During elongation and whipping, evaporation of some of the solvent also takes place which further reduces the diameter of the NFs. Using this simple ES process, NFs can be produced with a size range of a few micrometers to tens of nanometers. Generally, ES can be categorized as horizontal and vertical in practice. In horizontal type ES, the effective force is the charged force obtained by the applied voltage and the opposite attractive force in the collector, which pulls the NFs. In the vertical type, there are two forces that draw the NFs: the collector charge and the gravitational pull, which produces narrow NFs with a minimum diameter.[75]

In addition to the complex hydrodynamics involved in the ES process,[82,83] there are some process parameters that affect the final morphology of the NFs. Major process parameters include the viscosity and surface tension of the solution, applied voltage, feed rate, distance between the needle and collector, needle or nozzle size and the environment (humidity).

Metal oxides are not spinnable directly but it is possible from their melt at extremely high temperatures. Therefore, metal oxides need to rely on the use of precursor solutions. Fig. 2 presents a complete procedure for the fabrication of composite ceramic NFs by ES. The method consists of three major steps:

(i) Preparation of an organic precursor solution containing an alkoxide of metal or metal salt with a polymer matrix. Before preparing the solution, the compatibility and solubility of a certain metal oxide with a polymer solvent or precursor should be examined to achieve the required viscosity. Polyvinylpyrrolidone (PVP), polyvinyl acetate (PVAc), polyvinyl alcohol (PVA), polyacrylonitrile (PAN), and polyethylene oxide (PEO)[84] are the most common polymers used to prepare metal oxide composite NFs with the appropriate rheological properties.

(ii) ES of the prepared solution to produce the composite NFs, which also contain the polymer matrix or solvents. For metal oxide NFs, the ES process is usually carried out at room temperature in a controlled environment.

(iii) Calcination or sintering of electrospun NFs at elevated temperatures to obtain the desired crystalline NFs by the evaporation of all organic components. The diameter of the calcined NFs is generally smaller than the as-spun NFs due to the loss of the polymeric solvent during the calcination process. Moreover, extremely small grains, called nanograins, evolve on the NFs during the calcination process, which play a significant role in the resulting gas sensing properties of the NFs.

The size of the nanograins can be manipulated and changed according to the desired applications of the NFs by controlling the heat treatment conditions (heating temperature, heating time, heating rate, cooling rate). For gas sensing applications, the size of the nanograins must be optimized to obtain the best sensing performance. Generally, NFs with smaller nanograins have better sensitivity and a faster response than those with larger nanograins due to the higher surface area. Moreover, nanograins on NFs also influence their electrical transport, magnetic, optical, and photocatalytic properties in addition to their gas sensing properties.[85,86] A number of composite oxide-based NFs including CuO-SnO_2,[87] ZnO-CuO,[88] TiO_2-ZnO,[89,90] NiO-SnO_2,[91] ZnO-In_2O_3,[92,93] In_2O_3-WO_3,[94] La_2O_3-WO_3,[95] SnO_2-CeO_2,[96] SnO_2-In_2O_3,[97] and $In_{2-x}Ni_xO_3$,[98] have been prepared

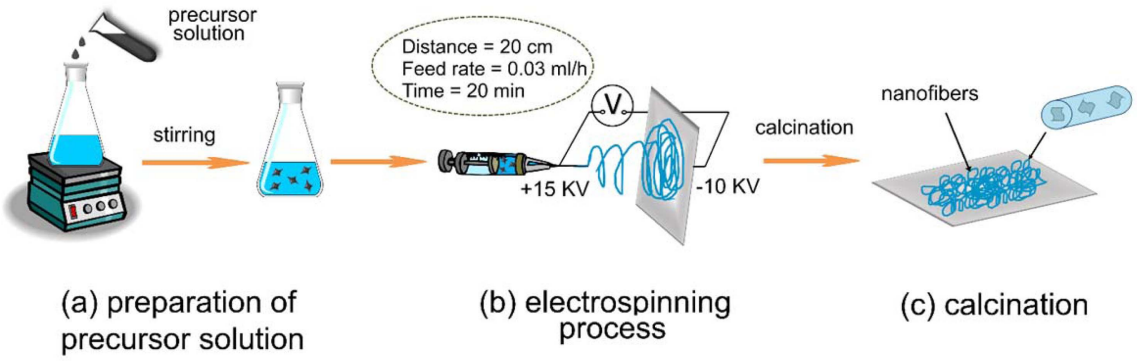

Fig. 2. Complete procedure for the production of composite ceramic NFs (After [59]).

by ES for gas sensing applications.

In the ES field, a notable breakthrough is the invention of the coaxial-ES technique by Sun *et al.*,[99] in which two or multi-coaxial capillaries have been used instead of the traditional single spinneret. Therefore, two or multi-fluids can be used for a core-shell (C-S) or more complicated compound jets in an electric field and then solidified to the desirable structures. In this process, two dissimilar materials are delivered independently through a co-axial capillary and drawn to generate NFs with a C-S configuration.[100] Thus far, coaxial ES have been exploited to produce different structures of NF, such as core-shell, hollow, and porous structures.[101] In addition, various types of fiber morphologies, are accessible by coaxial ES.[102] In coaxial ES, the reduced surface tension at the boundary of two fluids and the elasticity of the shell fluid delays or suppresses the Rayleigh instability of the core fluid, enabling NFs formation of the otherwise non-electrospinnable core materials.[103]

5. General Sensing Mechanisms

Although the sensing measurements of metal oxide-based gas sensors are simple in nature and only the variations of the resistance of the sensor are needed, the detection mechanism of gas sensors is a complex phenomenon that is still not completely understood. The complexity arises due to a range of factors, which include the adsorption ability, electrophysical and chemical properties, catalytic activity, thermodynamic stability, and adsorption/desorption properties of the surface.[104,105] Metal oxide-based gas sensors are broadly recognized as "chemiresistive" because of the change in their electrical conductance/resistance caused by the interaction with the target gas molecules.

As shown in Fig. 3, metal oxides are generally deposited on an insulating substrate, such as SiO_2 or alumina. Subsequently, interdigital electrodes for the measurements of the resistance are deposited on the substrate by a sputtering process using interdigitated electrode masks. The change in resistance of the metal oxide depends on the temperature of the sensor, nature of the target gas (oxidizing or reducing), and the type of the majority charge carriers. Those metal oxide semiconductors, in which the majority charge carriers are electrons, are classified as n-type semiconductors while p-type semiconductors are those in which the majority charge carriers are holes.

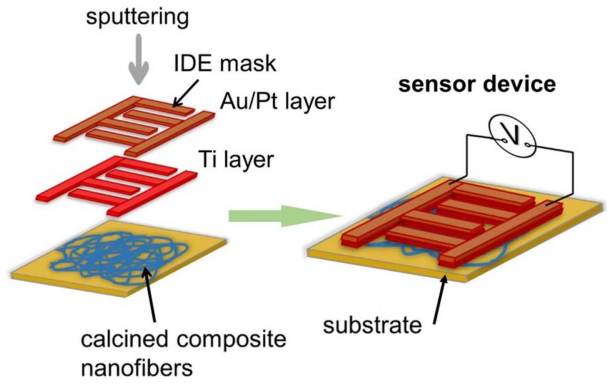

Fig. 3. Schematic representation of fabricating the composite NFs gas sensor (After [59]).

At temperatures of 100°C to 500°C, atmospheric oxygen interacts, adsorbs, and becomes ionized into atomic (O^-, O^{2-}) and molecular ions (O_2^-) by taking electrons from the surface of an n-type semiconductor. Generally, the molecular form dominates at temperatures below 150°C and the atomic form dominates at temperatures higher than 150°C.[106,107] This oxygen ionosorption leads to the formation of a region or layer with a smaller number of electrons near the surface of the semiconductor than its interior region. This electron-

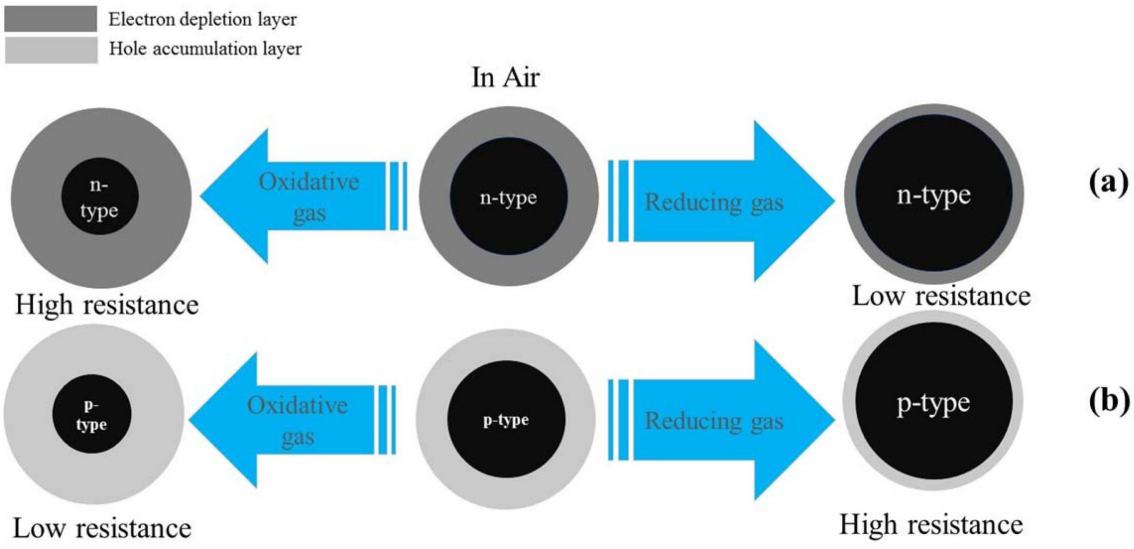

Fig. 4. Schematic diagram of the sensing mechanism in the presence of reducing and oxidative gas sensors; (a) n-type metal oxide semiconductors and (b) p-type metal oxide semiconductors.

depleted region or layer is called the electron depletion layer and can be understood by considering the electronic core-shell configuration of the NFs or nanograins of the semiconductor, as shown in Fig. 4(a) in air, where the resistive shell is the electron depletion layer and the semiconducting core is usually called the conduction channel because the flow of the electrons occurs mainly through the semiconducting core of the n-type metal oxide NFs. In the case of p-type semiconductors, however, the ionosorption of oxygen leads to the formation of a hole-accumulation layer near the surface of the NF (Fig. 4(b)) due to the interaction between the oppositely charged species, which again develops an electronic core-shell configuration in the NFs or nanograins. In this case, the resistive or insulating region is the core and the shell (which is the hole-accumulation layer) is semiconducting, which acts as a conduction channel.

The surface concentration of oxygen ions changes due to the interaction of an analyte gas with the semiconductor. The surface oxygen ion concentration on an n-type semiconductor decreases in the presence of a reducing gas due to their partial or complete oxidation, injecting the extracted electrons back to the semiconductor and decreasing the electron depletion layer thickness (Fig. 4(a)) and increasing the conductivity of the n-type semiconductor. An oxidizing gas increases the resistance of an n-type semiconductor by increasing the thickness of the electron depletion layer (Fig. 4(a)), whereas p-type oxide semiconductors show the opposite response. That is, their resistance increases and decreases in the presence of a reducing and oxidizing gas, respectively, due to the opposite effect of these gases on the surface concentration of oxygen ions and hence on the hole-accumulation layer (Fig. 4(b)).

The sensing properties of semiconducting materials are also influenced greatly by the grain size. A low sensitivity is expected if the grain size (D) is large enough so that the bulk region remains unaffected by surface reactions (i.e., $D >> \lambda$), where λ is the Debye length, which is typically in the range of 2-100 nm. A very high sensitivity is expected if $D \leq \lambda$ (i.e., the whole grain is depleted by the charge carriers and the surface reactions affect the entire grain/semiconductor).[108,109] The size of the nanograins on the NFs are usually less than the Debye length and the configuration of NFs is naturally in such a way that it is almost completely accessible to the analyte gas molecules. This increases their interactions with the semiconductor, which is advantageous for the design of highly sensitive gas sensors.

For composite NFs, there are two types of metal oxides. Suppose that two metal oxides (n-type and p-type) (Fig. 5(a)) are in intimate contact. To equate the Fermi levels, electrons will flow from the n-type metal oxide to the p-type metal oxide, resulting in band bending at the heterointerfaces (Fig. 5(b)). Upon exposure to the reducing gases and toxic gases, modulation of this heterointerface will cause a change in the resistance of the composite sensor and a high response. For the case of similar semiconducting type metal oxide composites such as n-n type composites, the work function (WF) difference between two metal oxides (Fig. 5(c)) will cause the band bending at interfaces in n-n metal oxides (Fig. 5(d)).

6. n-p Composite NFs Sensors

N-type metal oxide semiconductors are the most commonly used materials for gas sensing applications and are

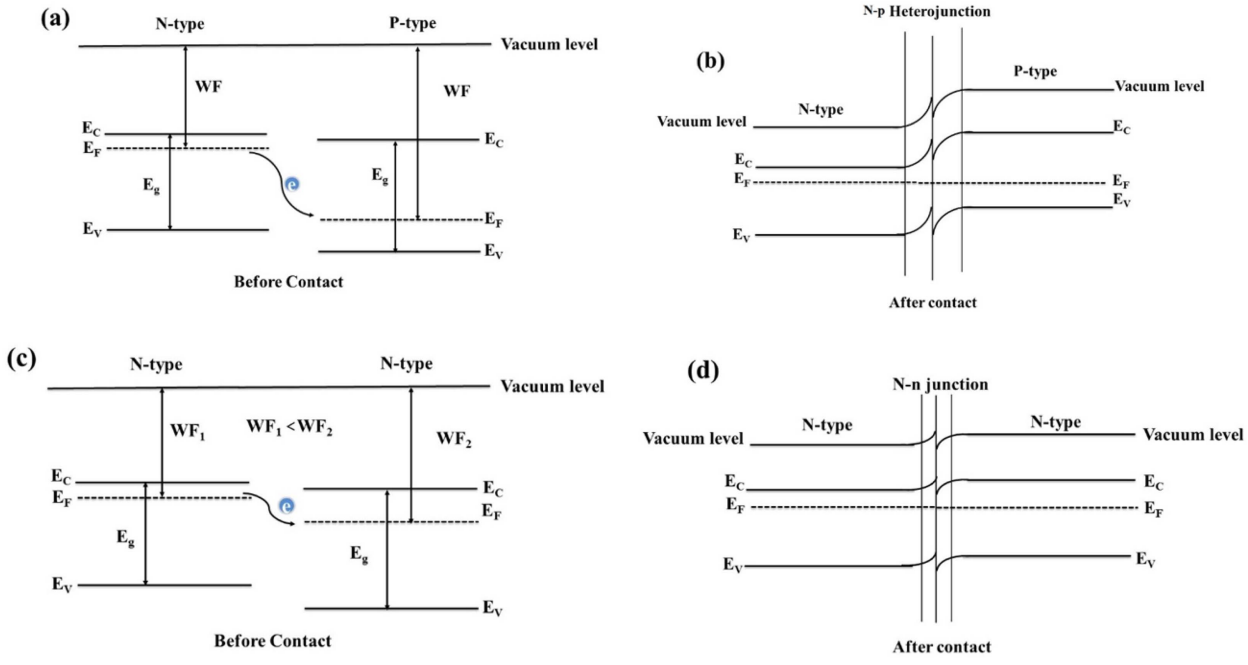

Fig. 5. Band structures of n-type and p-type metal oxides (a) before and (b) after intimate contact. Band structures of two n-type metal oxides (c) before and (d) after intimate contact.

still used in most commercialized gas sensors because of their higher sensitivity than p-type oxide semiconductors. The response of an n-type metal oxide gas sensor (R_n) is equal to the square of that of a p-type metal oxide gas sensor (R_p), provided that both sensors have identical morphological configurations, as follows:[110]

$$R_n = R_p^2 \quad (1)$$

Accordingly, considerable efforts have been made to enhance the sensitivity of p-type metal oxide-based gas sensors. Despite their shortcomings, most p-type oxides semiconductor-based gas sensors have potential for practical applications, such as promoting the selective oxidation of various volatile organic compounds.[26] Moreover, p-type metal oxide semiconductors are being applied to develop ultra-sensitive chemiresistive gas sensors by tuning the electrical properties of the n-type sensing materials by forming p-n heterojunctions or p-n heterointerfaces. In n-p composite NFs, the sensing mechanisms are explained by the nature and number of interfaces between the composite materials. These n-p heterointerfaces among the nanograins of the NFs play a substantial role in enhancing the sensitivity of the metal oxide composites.

p-n composites are the most common composites among metal oxide semiconductor-based gas sensors. These interfaces produce the resistance modulation in the NFs, in addition to the resistance modulation caused by homointerfaces and radial resistance modulation present in pristine NFs.

Table 1 lists some of the highly sensitive p-n composite NFs reported thus far. Wang *et al.*[111] prepared n-ZnO and p-Cr_2O_3 (3.0 wt.%, 4.5 wt.%, and 8.5 wt.%) composite NFs by ES and tested them for the detection of low concentrations of ethanol. They reported that the NF with the 4.5 wt.% Cr_2O_3 loading showed the best response to 1 ppm ethanol with response and recovery times of 1 s and 5 s, respectively. In the presence of heterointerfaces, the initial resistance of the sensors is relatively higher compared to the pristine ZnO NFs sensor. In the presence of an oxidative gas, such as NO_2, the additional increase in resistance is negligible. On the other hand, with the introduction of a reducing gas, such as ethanol, a large decrease in the resistance is possible due to the initial high resistance of the p-n heterojunction sensor, and a strong response is observed.

The C-S configuration is a fascinating nanocomposite for gas sensing applications because the interfaces are maximized in this special configuration. In this regard, Katoch *et al.*[88] prepared n-ZnO/p-CuO NFs with a C-S configuration for the detection of very low concentrations of reducing gases. In p/n C-S NFs, if the shell thickness is equivalent to Debye length of the shell material, the shell layer will be completely depleted and the sensor shows a higher response when the shell thickness is less than Debye length. The Debye length for the ZnO thin films grown by the ALD technique, at 300°C is estimated to be ~22 nm. Accordingly, in pCuO/nZnO C-S NFs, the ZnO shell layer had a depletion layer of approximately 22 nm. The CO gas sensing properties were examined as a function of the ZnO shell layer thickness, and it was reported that the response reaches a maximum for the p/n C-S NFs with a 16 nm thick shell. This suggests that the p/n C-S NFs with the 16 nm thic shell were fully depleted, whereas the shells thicker than Debye length were partially depleted, therefore a higher response was observed for the p/n C-S NFs with a 16 nm thick shell.

Similarly, the CuO-SnO_2 composite NFs with different nanograin sizes were prepared for H_2S gas sensing.[87] The

Table 1. Some Sensing Properties of n-p Heterojunction Composite Electrospun Metal Oxide NFs Reported in the Literature

Material	Gas	Conc. (ppm)	T (°C)	Response (R_a/R_g)	Ref
ZnO-rGO	NO_2	5	400	119	[59]
CuO-SnO_2	H_2S	10	300	25799	[87]
CuO-ZnO	CO	0.1	300	7	[88]
p-NiO/n-SnO_2	H_2	100	320	13.5	[91]
La_2O_3-WO_3	Acetone	0.8	350	1.8	[95]
SnO_2-CeO_2	H_2S	20	210	90	[96]
$In_{2-x}Ni_xO_3$	Ethanol	100	180	80	[98]
ZnO-CuO	H_2S	10	150	4489.9	[133]
SnO_2-RGO	CO	1	200	10	[117]
4.5 wt.% Cr_2O_3-ZnO	Ethanol	100	300	24	[111]
p-In_2O_3/TiO_2	NO_x	97	25	40	[134]
α-Fe_2O_3@NiO	HCHO	50	240	12.8	[135]
p-$La_{0.67}Sr_{0.33}MnO_3$/n-CeO_2	Propane	20	800	75	[136]
p-NiO/n-ZnO	Trimethylamine	100	260	892	[137]
NiO-SnO_2	Toluene	50	330	11	[138]
CuO-loaded In_2O_3	H_2S	5	RT	9170	[139]
NiO-doped SnO_2	Formaldehyde	10	200	6.3	[140]

size of the nanograins was controlled by controlling the heat treatment or calcination conditions. NFs with a smaller nanograin size showed stronger responses than those with larger nanograins. The authors attributed this to the large number of heterointerfaces between CuO and SnO_2 smaller nanograins. Moreover, the high sensitivity of the composite NFs, particularly towards H_2S, was attributed to the transformation of p-CuO to metallic CuS in the presence of H_2S.

Recently, graphene has attracted considerable attention for gas sensing applications. Graphene has unique properties, such as a huge surface area to volume ratio, excellent electrical and thermal conductivity, low electronic noise, and high chemical stability.[112] Schedin *et al.*[113] reported the gas sensing properties of graphene and showed that graphene could detect individual gas molecules because of its low electronic noise. Nevertheless, graphene gas sensors have no sufficient sensitivity to the target gases and its alternative form, reduced graphene oxide (rGO), is more beneficial for gas sensing applications[114-116] because of its abundance of oxygen functional groups that provide an increased number of adsorption sites.

The gas sensing behavior of rGO-loaded composite NFs have been investigated. Lee *et al.*[117] and Ul abideen *et al.*[59] used p-type rGO nanosheets (0.04 - 1.04 wt.%) in SnO_2 NFs and ZnO, respectively. The rGO nanosheets had no effect on the size or shape of the nanograins while they enhanced the sensing properties of both SnO_2 and ZnO NFs significantly compared to their pristine SnO_2 and ZnO sensors. In both cases, the optimal amount of rGO was found to be 0.44 wt.%. The enhanced sensing properties of the rGO-loaded composite NFs were mainly attributed to the formation of local p-n heterojunctions among the p-rGO nanosheets and SnO_2 and ZnO NFs grains, which was revealed by TEM analysis. Fig. 6 shows the sensing mechanism for the rGO loaded ZnO composite NFs. p-rGO nanosheets formed p-n heterojunctions and acted as electron acceptors, thereby producing additional potential barriers in addition to the potential barriers present between the homojunctions or nanograins of SnO_2 or ZnO. The potential barriers formed at the p-n heterojunctions was the additional resistance modulation on the adsorption or desorption of gas molecules. Moreover, rGO nanosheets played a catalytic role in enhancing the gas reaction with the sensing material by acting as an electron acceptors. In another study, Ul abidden *et al.*[118] prepared rGO-loaded ZnO NFs by ES and it was reported that the fabricated sensor was ultra-sensitive to very low concentrations of H_2 gas with rapid recovery times. The response (R_a/R_g) to 100 ppb of H_2 gas was 866. The extraordinary sensing performance was attributed to the combined effect of hydrogen-induced metallization of the ZnO surface and the presence of rGO nanosheets along with the ZnO nanograins. Wang *et al.*,[119] reported the enhanced HCHO sensing properties of electrospun hollow SnO_2 NFs by graphene oxide (GO). The optimal loading was 1 wt.% GO and the response of SnO_2-GO sensor towards 100 ppm HCHO at 120°C was 32, which was 4 times higher

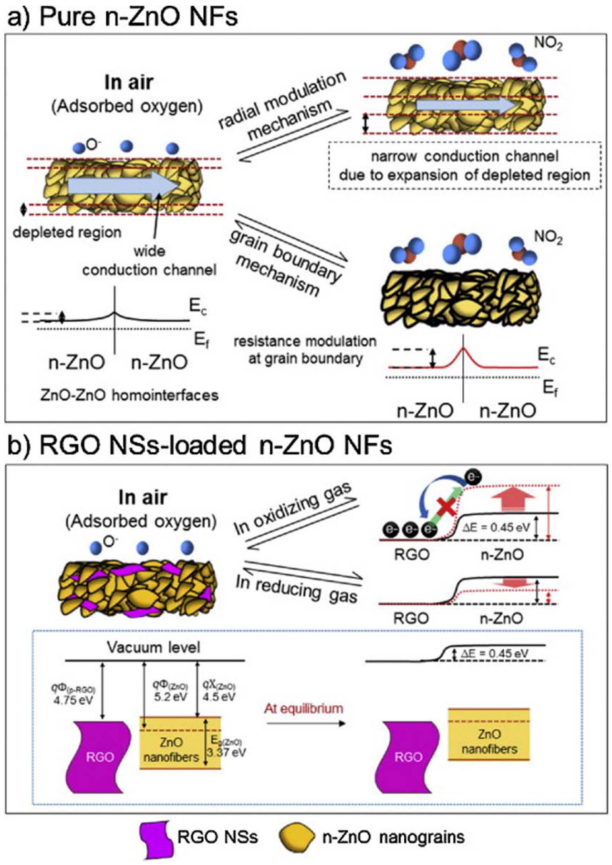

Fig. 6. Schematic diagram of the sensing mechanisms involved in (a) pure ZnO NFs (b) RGO-loaded ZnO composite NFs (After [59]).

than that of the pristine hollow SnO_2 NFs. The enhanced gas sensing properties were attributed to the synergistic effects of the hollow SnO_2 NFs and GO nanosheet network, including formation of n-p heterojunctions, large specific surface area, rich functional groups, and the electric regulation effects of GO.

7. n-n Heterojunction Composite NFs

Additional potential barriers and band bending can also occur at the n-n and p-p interfaces. In n-p heterointerfaces, the resistance increases due to the smaller number of electrons due to electron-hole recombination, while in n-n heterointerfaces, the number of electrons is greater and they flow from a higher energy conduction band to a lower energy conduction band, forming an accumulation layer instead of a depletion layer.[41,120] The accumulation layer can be depleted by oxygen adsorption, which increases the potential barriers at the interfaces and enhances the response. Many studies have reported n-n type composite NFs. Table 2 lists some of reported papers in this field. Lee *et al.*[93] reported a highly selective and sensitive n-n type gas sensor composed of ZnO-In_2O_3 composite NFs for trimethylamine gas. The composite NFs showed stronger responses to trimethylamine

Table 2. Some **S**ensing Properties of n-n Heterojunction Composite Electrospun Metal Oxide NFs Reported in the Literature

Material	gas	Conc. (ppm)	T (°C)	Response (R_a/R_g)	Ref
TiO_2-ZnO	O_2	10000	300	20	[89]
TiO_2/ZnO	CO	0.1	375	15.2	[90]
In_2O_3/ZnO bi-layer	C_2H_5OH	100	210	25	[92]
ZnO/In_2O_3/ZnO tri-layer	C_2H_5OH	100	210	17	[92]
ZnO-In_2O_3	C_3H_9N	5	375	119.4	[93]
In_2O_3-WO_3	C_3H_6O	0.4	275	1.3	[94]
SnO_2/In_2O_3	HCHO	0.5	375	2.2	[97]
SnO_2-ZnO	CO	10	350	11	[141]
SnO_2/MWCNT	CO	50	25	1.29	[142]
Polyaniline/TiO_2	NH_3	25 ppb	25	0.41	[143]
SnO_2-ZnO	CH_3OH	10	350	8.5	[144]
Polypyrrole-WO_3	NH_3	20	100	26	[145]
Sn-SnO_2/Carbon	C_2H_5OH	500	240	30	[146]
ZnO-TiO_2	C_2H_5OH	500	320	50.6	[147]
$La_{0.7}Sr_{0.3}FeO$-In_2O_3-SnO_2	C_3H_9N	1	80	8	[148]
SnO_2-In_2O_3	NH_3	1	25	21	[149]
Al_2O_3- In_2O_3	NO_x	97	25	100	[126]
SnO_2/α-Fe_2O_3	C_3H_6O	100	340	30.363	[150]

than pristine ZnO and pristine In_2O_3 NFs. The maximum response to 5 ppm trimethylamine of the ZnO-In_2O_3 composite NFs with (Zn) : (In) = 67 : 33 in at.% was 133.9 at 300°C. The high sensitivity was attributed to the conduction and chemiresistive variations at the heterointerfaces, which in turn was due to the difference in the work functions of ZnO (4.45 eV)[121] and In_2O_3 (5.0 eV).[122]

Similarly, Zhang *et al.*[92] reported the high sensitivity and rapid responses of ZnO-In_2O_3 NFs. They compared the responses of pristine ZnO NFs with the ZnO-In_2O_3 bi-layer and ZnO-In_2O_3-ZnO tri-layer composite NFs. The composite NFs showed stronger responses compared to pure ZnO NFs but the best responses (response of 25 to 100 ppm ethanol at 210°C) were achieved by the ZnO-In_2O_3 bi-layer composite NFs with response and recovery times of approximately 2 s and 1 s, respectively. The high sensing performance of ZnO-In_2O_3 was related to the web-like structure, large surface area to volume ratio of the NFs, and the heterojunctions formed by the double-layer structure. The heterojunctions between the NFs hindered electron flow by forming a depletion layer at the heterojunctions.[123,124] The decreased sensitivity of ZnO-In_2O_3-ZnO was related to the high film thickness compared to the ZnO-In_2O_3 bi-layer, which may limit the signal transmission from the film surface to the electrodes,[125] leading to a decrease in the film performance.

Room temperature sensing is of importance for sensing devices because it greatly decreases the power consumption of the device. Gao *et al.*[126] reported the significant NO_x gas sensing performances of mesoporous electrospun Al_2O_3-In_2O_3 composite NFs at room temperature. The Al_2O_3-In_2O_3 NFs containing 20 at.% Al_2O_3 exhibited a strong response of 100 to 97 ppm NO_x with a detection limit of 291 ppb and high stability to 0.97 - 9.7 ppm NO_x. The enhanced gas sensing was attributed to the synergistic effects between mesoporous NFs and the modifying role of Al_2O_3. The mesopores and unique 1D hollow structure with a high surface-to-volume ratio provided channels for gas adsorption-desorption and diffusion, thereby providing more accessible active sites for the reaction of NO_x with surface adsorbed oxygen ions. In addition, the Al_2O_3 additive increased the oxygen vacancy/defect and donor densities, controlled the grain growth and resistivity, and provided more active sites for gas adsorption.

Katoch *et al.*[90] assessed TiO_2/ZnO composite hollow NFs for gas sensing applications. The TiO_2/ZnO layers were deposited by atomic layer deposition technique on sacrificial polymer NFs prepared by ES. The hollow NFs were produced by removing the polymer NFs by thermal heat treatment. The gas sensing characteristics were examined as a function of the outer ZnO layer to NO_2 and CO gases as representatives of oxidizing and reducing gases, respectively. The composite hollow NFs showed better sensitivity to CO gas compared to NO_2. The strong response to CO gas was explained in terms of the work function difference between TiO_2 and ZnO. The TiO_2 layer abstracted electrons from the ZnO layer, making it more depleted and resistive, and upon the reaction of CO with adsorbed oxygen species, electrons were released back to the surface of the sensors, resulting in a strong response to CO. In contrast, for NO_2 gas, not enough electrons could be abstracted by NO_2, resulting in a weak response.

In another study, Li *et al.*[127] synthesized electrospun hollow ZnO-SnO_2 core-shell NFs for ethanol sensing. At 200°C, the response of the hollow C-S ZnO-SnO_2 sensor towards

100 ppm ethanol was 392.29, which was 11 times larger than those of the SnO_2 sensor. The response and recovery times of the ZnO-SnO_2 sensor were 75 s and 12 s, whereas that of the SnO_2 sensor was 86 s and 14 s, respectively. The excellent sensing performance was attributed to the unique hollow structure, oxygen vacancies, and the n-n heterojunction, which was generated at the interface between ZnO and SnO_2. Furthermore, they reported that a small amount of Zn^{2+} ions may diffuse into the lattice of SnO_2 and replace the Sn^{4+} sites during the hydrothermal process. As a result, the concentration of oxygen vacancies increased by substitution of Zn^{2+} for Sn^{+4}. These oxygen vacancies acted as an electron donor, and enhanced the adsorption of atmospheric oxygen on the surface of sensor.

Plasma treatment is an effective method for modifying the properties of nanomaterials. Using this technique, it is possible to modify the surface properties of NFs without affecting the bulk properties. In this regards, Du *et al.*,[128] reported the HCHO sensing properties of electrospun SnO_2/In_2O_3 composite hetero-NFs treated with oxygen plasma in a radio frequency (RF) plasma treatment chamber at low temperatures. The gas sensors of treated SnO_2/In_2O_3 composite NFs exhibit strong and rapid response and recovery times to HCHO, and the sensor showed good selectivity to HCHO. The enhanced gas response was attributed to the increasing conducting electron concentrations, porosity, and specific surface area after treatment with oxygen plasma.

8. Noble Metal-Metal Oxide Composite NFs

To further enhance the sensitivity and lower the operating temperature of the composite gas sensors, noble metal nanoparticles (NPs) can be added to NFs as promoters or activators. In 1983, Yamazoe *et al.*[28,30] proposed two types of sensitization mechanisms for enhancing the sensing response of gas sensors due to the presence of noble metals NPs: (i) chemical sensitization and (ii) electronic sensitization, as shown in Fig. 7. In chemical sensitization, additives promote the chemical reaction between the sensing material and the target gas by a spill-over effect, whereas in electronic sensitization, the change in the oxidation state of noble metal NPs occurs because of the electronic interaction, i.e., the noble metal acts as an electron donor or acceptor on the surface of the sensing material.

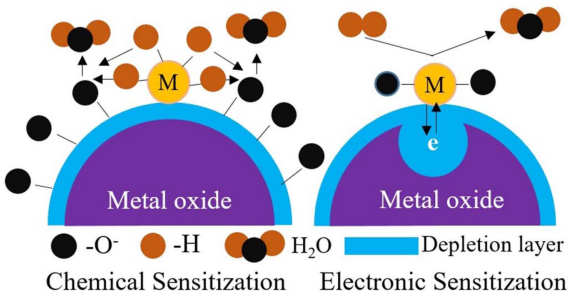

Fig. 7. Chemical and electronic sensitizations in noble metal-functionalized metal oxide NFs (Adopted from [30]).

Noble metals possess high electrical conductivity to facilitate rapid electron transfer and catalyze the oxidation of reducing gas molecules. In addition, metal oxide NFs have a large specific surface area to provide efficient catalytic particle dispersion, a high capacity for storing and releasing oxygen, and a porous structure to promote gas flow. Therefore, combining the excellent features of 1D metal oxide NFs and the outstanding catalytic oxidation activity of noble metals NPs has promising effects for gas sensing applications. In particular, noble metals promote gas sensing reactions by reducing the activation energy, and increase the sensing response and selectivity while also decreasing the maximum working temperature of the sensors.[129]

Because metal oxides generally have a lower work function than metals, upon intimate contact of the metal oxide with noble metals, electrons will transfer from metal oxides to the noble metals, resulting in contraction of conduction channels inside the metal oxide NFs. Accordingly, upon exposure to target gases a larger change in the diameter of conduction channel will result in a higher response in noble metal decorated metal oxide NFs relative to pristine metal oxide NFs. Fig. 8 schematically shows the positive effect of noble metals. A comparison between the conduction channels of pristine and noble metal decorated metal oxide sensors (Figs. 8(a) and (b)), show that the diameter of conduction channel decreases significantly in the presence of noble metal NPs. When the sensors are exposed to the reducing gas, the diameter of conduction channel in both pristine and noble metal decorated metal oxide NFs sensors increases (Figs. 8(c) and (d)). However, the ratio of changes in the diameter of conduction channel in air and the reducing gas atmosphere is larger than the case of pristine metal oxide NF sensor.

Lin *et al.*[130] prepared electrospun Pd NPs-decorated hollow SnO_2 NFs and examined their HCHO sensing properties. Compared to the pristine SnO_2 NFs gas sensor, the optimal operating temperature of Pd-decorated hollow SnO_2 NFs gas sensor decreased to 160°C from 180°C and the response to 100 ppm HCHO increased to 18.8 from 5.4. Moreover, the response and recovery times were shortened

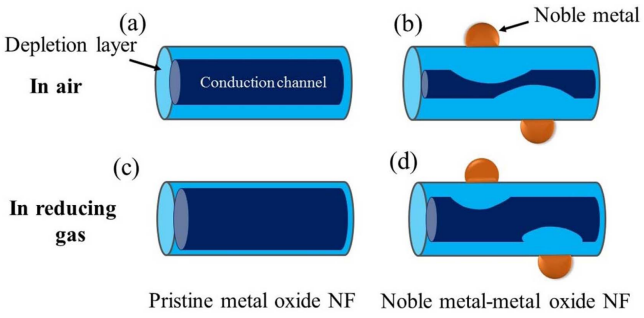

Fig. 8. Change of conduction channel in metal oxide NFs due to presence of noble metal; (a) pristine metal oxide NF in air, (b) noble metal-metal oxide NF in air, (c) pristine metal oxide NF in reducing gas atmosphere, and (d) noble metal-metal oxide NF in reducing gas atmosphere.

considerably. The strong sensing performance was attributed to the hollow structure of the sensor, formation of Schottky barriers, and the spillover effect of Pd NPs. In another study, Xu *et al.*[131] reported the acetone gas sensing properties of Ag-decorated SnO_2 hollow NFs. The sensor could detect the 5 ppm acetone. The high sensing performance was attributed to the unique 1D hollow nanostructure, the outstanding catalytic oxidation activity of Ag NPs, and the p-n heterointerface formed between p-type Ag_2O and n-type SnO_2.

The WO_3 NFs for gas sensing studies are rarely reported. Yong *et al.*[129] reported Au-functionalized WO_3 composite NFs by ES for the sensing of n-butanol. The enhanced response of the WO_3-Au composite NF sensor toward n-butanol was related to the excellent catalytic activity of the Au NPs, which enhanced the oxygen molecule to an ion conversion rate and the existence of multiple depletion layers at the surface of the WO_3-Au composite NFs, which resulted in a larger change in resistance upon exposure to n-butanol. In another study, Kim *et al.*[132] showed a detection limit of 20 ppb with a gas response of 1.32 towards toluene at 350°C by Pd NP-embedded WO_3 NFs for the possible detection of lung cancer.

9. Conclusions and Future Outlooks

This review explained the ES principles for the synthesis of NFs and showed that composite metal oxide electrospun NF-based gas sensors have great potential for sensing applications for the detection of toxic gases. Different composite NFs systems, such as n-p and n-n composite heterojunctions, as well as noble metal-metal oxide composite NFs were discussed. The enhanced gas response in the composite NFs was attributed to the high surface area, presence of many grain boundaries, the existence of heterojunctions in n-p and n-n composite NFs, and the promotional role of noble metals in terms of chemical and electronic sensitization. By morphological engineering of NFs, different structures, such as hollow NFs, C-S NFs, and hollow C-S NFs can be synthesized by the ES method. These structures show very good sensing performance and can detect sub-ppm concentrations of toxic gases.

Because the NFs area is a rapidly growing field with many applications, in addition to gas sensors, it is expected that by the design of new ES set-ups, more complex composite NFs could be synthesized with larger surface areas, more porous structures and more heterojunctions. These properties will allow the fabrication of novel high performance gas sensors.

Acknowledgments

This study was supported by Basic Science Research Program through the National Research Foundation of Korea (NRF) funded by the Ministry of Education (2016R1D1A1B03935228).

REFERENCES

1. A. Mirzaei, S. G. Leonardi, and G. Neri, "Detection of Hazardous Volatile Organic Compounds (VOCs) by Metal Oxide Nanostructures-Based Gas Sensors: A Review," *Ceram. Int.*, **42** [14] 15119-41 (2016).
2. G. Korotcenkov and B. K. Cho, "Metal Oxide Composites in Conductometric Gas Sensors: Achievements and Challenges," *Sens. Actuators, B,* **244** 182-210 (2017).
3. I. Fratoddi, I. Venditti, C. Cametti, and M. V. Russo, "Chemiresistive Polyaniline-Based Gas Sensors: A Mini Review," *Sens. Actuators, B,* **220** 534-48 (2015).
4. A. Mirzaei and G. Neri, "Microwave-Assisted Synthesis of Metal Oxide Nanostructures for Gas Sensing Application: A Review," *Sens. Actuators, B,* **237** 749-75 (2016).
5. S. S. Varghese, S. Lonkar, K. K. Singh, S. Swaminathan, and A. Abdala, "Recent Advances in Graphene Based Gas Sensors," *Sens. Actuators, B,* **218** 160-83 (2015).
6. M. Kampa and E. Castanas, "Human Health Effects of Air Pollution," *Environ. Pollut.*, **151** [2] 362-7 (2008).
7. I. Simon, N. Bârsan, M. Bauer, and U. Weimar, "Micromachined Metal Oxide Gas Sensors: Opportunities to Improve Sensor Performance," *Sens. Actuators, B,* **73** [1] 1-26 (2001).
8. A. D. McNaught and A. Wilkinson, Compendium of Chemical Terminology; Vol. 1669, pp. 165-66, Blackwell Science, Oxford, 1997.
9. G. Eranna, Metal Oxide Nanostructures as Gas Sensing Devices; Vol. 316, pp. 1-2, CRC Press, Boca Raton, 2011.
10. V. K. Khanna, Nanosensors: Physical, Chemical, and Biological; Vol. 53, pp. 51-522, CRC Press, Oxford, 2011.
11. W. P. Jakubik, "Surface Acoustic Wave-Based Gas Sensors," *Thin Solid Films*, **520** [3] 986-93 (2011).
12. F. Tavoli, N. Alizadeh, "Optical Ammonia Gas Sensor Based on Nanostructure Dye-Doped Polypyrrole," *Sens. Actuators, B,* **176** 761-67 (2013).
13. C. H. Han, D. W. Hong, I. J. Kim, J. Gwak, S. D. Han, and K. C. Singh, "Synthesis of Pd or Pt/Titanate Nanotube and Its Application to Catalytic Type Hydrogen Gas Sensor," *Sens. Actuators, B,* **128** 320-25 (2007).
14. F. Tebizi-Tighilt, F. Zane, N. Belhaneche-Bensemra, S. Belhousse, S. Sam, and N. Gabouze, "Electrochemical Gas Sensors Based on Polypyrrole-Porous Silicon," *Appl. Surf. Sci.*, **269** 180-83 (2013).
15. G. Barochi, J. Rossignol, and M. Bouvet, "Development of Microwave Gas Sensors," *Sens. Actuators, B,* **157** [2] 374-79 (2011).
16. M. J. Madou and S. R. Morrison, Chemical Sensing with Solid State Devices; pp. 163-66, Academic Press, New York, 1989.
17. A. Mirzaei, K. Janghorban, B. Hashemi, and G. Neri, "Metal-Core@ Metal Oxide-Shell Nanomaterials for Gas-Sensing Applications: A Review," *J. Nanopart. Res.*, **9** [17] 1-36 (2015).
18. C. G. B. Garrett and W. H. Brattain, "Physical Theory of Semiconductor Surfaces," *Phys. Rev.*, **99** 376-87 (1955).
19. W. H. Brattain and C. G. B. Garrett, "Surface Properties of Semiconductors," *Physica*, **20** 885-92 (1954).
20. W. H. Brattain and J. Bardeen, "Surface Properties of

Germanium," *Bell Syst. Tech. J.*, **32** 1-41 (1953).
21. A. Bielański, J. Dereń, and J. Haber, "Electric Conductivity and Catalytic Activity of Semiconducting Oxide Catalysts," *Nature*, **179** 668-9 (1957).
22. T. Seiyama, A. Kato, K. Fujiishi, and M. Nagatani, "A New Detector for Gaseous Components Using Semiconductive Thin Films," *Anal. Chem.*, **34** 1502-3 (1962).
23. T. Seiyama and S. Kagawa, "Study on a Detector for Gaseous Components Using Semiconductive Thin Films" *Anal. Chem.*, **38** 1069-73 (1966).
24. N. Taguchi, "Method for Making a Gas-Sensing Element"; US Patent 3,625,756 (December 7, 1971).
25. N. Taguchi, "Semiconductor Gas Detecting Device"; US Patent 3,732,519 (May 8, 1973).
26. H. J. Kim and J. H. Lee, "Highly Sensitive and Selective Gas Sensors Using p-Type Oxide Semiconductors: Overview," *Sens. Actuators, B,* **192** 607-27 (2014).
27. S. R. Morrison, "Selectivity in Semiconductor Gas Sensors," *Sens. Actuators, B,* **12** 425-40 (1987).
28. N. Yamazoe, Y. Kurokawa, and T. Seiyama, "Effects of Additives on Semiconductor Gas Sensors," *Sens. Actuators, B*, **4** 283-9 (1983).
29. N. Yamazoe, "Toward Innovations of Gas Sensor Technology," *Sens. Actuators, B,* **108** 2-14 (2005).
30. N. Yamazoe, G. Sakai, and K. Shimanoe, "Oxide Semiconductor Gas Sensors," *Catal. Surv. Asia*, **7** [1] 63-75 (2003).
31. N. Yamazoe, "New Approaches for Improving Semiconductor Gas Sensors," *Sens. Actuators, B,* **5** 7-19 (1991).
32. A. Khayatian, S. Safa, R. Azimirad, M. A. Kashi, and S. F. Akhtarianfar, "The Effect of Fe-Dopant Concentration on Ethanol Gas Sensing Properties of Fe Doped ZnO/ZnO Shell/Core nanorods," *Phys. E*, **84** 71-8 (2016).
33. X. Kou, C. Wang, M. Ding, C. Feng, X. Li, J. Ma, H. Zhang, and Y. Sun, "Synthesis of Co-Doped SnO_2 Nanofibers and Their Enhanced Gas-Sensing Properties," *Sens. Actuators, B,* **236** 425-32 (2016).
34. K. G. Girija, K. Somasundaram, A. Topkar, and R. K. Vatsa, "Highly Selective H_2S Gas Sensor Based on Cu-Doped ZnO Nanocrystalline Films Deposited by RF Magnetron Sputtering of Powder Target," *J. Alloys Compd.*, **684** 15-20 (2016).
35. M. Epifani, J. Arbiol, E. Pellicer, E. Comini, P. Siciliano, G. Faglia, "Synthesis and Gas-Sensing Properties of Pd-Doped SnO_2 Nanocrystals. A Case Study of a General Methodology for Doping Metal Oxide Nanocrystals," *Cryst. Growth Des.*, **8** [5] 1774-8 (2008).
36. M. Epifani, T. Andreu, R. Zamani, J. Arbiol, E. Comini, and P. Siciliano, "Pt Doping Triggers Growth of TiO_2 Nanorods: Nanocomposite Synthesis and Gas-Sensing Properties," *CrystEngComm*, **14** 3882-87 (2012).
37. V. Dobrokhotov, D. N. Mcilroy, M. G. Norton, A. Abuzir, W. J. Yeh, and I. Stevenson, "Principles and Mechanisms of Gas Sensing by GaN Nanowires Functionalized with Gold Nnanoparticles," *J. Appl. Phys.*, **99** [10] 104302-9 (2006).
38. A. Kolmakov, D. O. Klenov, Y. Lilach, S. Stemmer, and M. Moskovits, "Enhanced Gas Sensing by Individual SnO_2 Nanowires and Nanobelts Functionalized with Pd Catalyst Particles," *Nano Lett.*, **5** [4] 667-73 (2005).
39. U. Heiz and E. L. Bullock, "Fundamental Aspects of Catalysis on Supported Metal Clusters," *J. Mater. Chem.*, **14** [4] 564-77 (2004).
40. W. C. Conner and J. L. Falconer, "Spillover in Heterogeneous Catalysis," *Chem. Rev.*, **95** [3] 759-88 (1995).
41. D. R. Miller, S. A. Akbar, and P. A. Morris, "Nanoscale Metal Oxide-Based Heterojunctions for Gas Sensing: A Review," *Sens. Actuators, B,* **204** 250-72 (2014).
42. E. Comini, M. Ferroni, V. Guidi, G. Faglia, G. Martinelli, and G. Sberveglieri, "Nanostructured Mixed Oxides Compounds for Gas Sensing Applications," *Sens. Actuators, B*, **84** 26-32 (2002).
43. D. Barreca, E. Comini, A. P. Ferrucci, A. Gasparotto, C. Maccato, and C. Maragno, "First Example of ZnO-TiO_2 Nanocomposites by Chemical Vapor Deposition: Structure, Morphology, Composition, and Gas Sensing Performances," *Chem. Mater.*, **19** [23] 5642-9 (2007).
44. C. W. Na, H. S. Woo, I. D. Kim, and J. H. Lee, "Selective Detection of NO_2 and C_2H_5OH Using a Co_3O_4-Decorated ZnO Nanowire Network Sensor," *Chem. Commun.*, **47** [18] 5148-50 (2011).
45. J. Zhang, X. Liu, L. Wang, T. Yang, X. Guo, and S. Wu, "Synthesis and Gas Sensing Pproperties of Alpha-Fe_2O^3@ZnO Core-Shell Nanospindles," *Nanotechnology*, **22** [18] 185501-8 (2011).
46. A. P. Lee and B. J. Reedy, "Temperature Modulation in Semiconductor Gas Sensing," *Sens. Actuators, B,* **60** 35-42 (1999).
47. A. Fort, M. Gregorkiewitz, N. Machetti, S. Rocchi, B. Serrano, and L. Tondi, "Selectivity Enhancement of SnO_2 Sensors by Means of Operating Temperature Modulation," *Thin Solid Films*, **418** [1] 2-8 (2002).
48. M. E. Franke, T. J. Koplin, and U. Simon, "Metal and Metal Oxide Nanoparticles in Chemiresistors: Does the Nanoscale Matter?," *Small*, **2** [1] 36-50 (2006).
49. Y. Shimizu and M. Egashira, "Basic Aspects and Challenges of Semiconductor Gas Sensors," *MRS Bull.*, **24** [6] 18-24 (1999).
50. J. H. Kim, A. Mirzaei, H. W. Kim, and S. S. Kim, "Extremely Sensitive and Selective Sub-ppm CO Detection by the Synergistic Effect of Au Nanoparticles and Core-Shell Nanowires," *Sens. Actuators, B,* **249** 177-88 (2017).
51. A. A. Mane and A. V. Moholkar, "Orthorhombic MoO_3 Nanobelts Based NO_2 Gas Sensor," *Appl. Surf. Sci.*, **405** 427-40 (2017).
52. L. Xue, W. Wang, Y. Guo, G. Liu, and P. Wan, "Flexible Polyaniline/Carbon Nanotube Nanocomposite Film-Based Electronic Gas Sensors," *Sens. Actuators, B,* **244** 47-53 (2017).
53. L. Liu, P. Song, Z. Yang, and Q. Wang, "Highly Sensitive and Selective Trimethylamine Sensors Based on WO_3 Nanorods Decorated with Au Nanoparticles," *Phys. E*, **90** 109-15 (2017).
54. J. H. Kim, J. H. Lee, A. Mirzaei, H. W. Kim, and S. S. Kim, "Optimization and Gas Sensing Mechanism of n-SnO_2-p-Co_3O_4 Composite Nanofibers," *Sens. Actuators, B,* **248** 500-11 (2017).
55. Z. L. Wang, "Characterizing the Structure and Properties of Individual Wire-Like Nanoentities," *Adv. Mater.*, **12**

[17] 1295-8 (2000).
56. J. D. Prades, R. Jimenez-Diaz, F. Hernandez-Ramirez, S. Barth, A. Cirera, and A. Romano-Rodriguez, "Ultralow Power Consumption Gas Sensors Based on Self-Heated Individual Nanowires," *Appl. Phys. Lett.*, **93** [12] 123110-13 (2008).
57. E. Comini, C. Baratto, I. Concina, G. Faglia, M. Falasconi, and M. Ferroni, "Metal Oxide Nanoscience and Nanotechnology for Chemical Sensors," *Sens. Actuators, B,* **179** 3-20 (2013).
58. E. Comini, C. Baratto, G. Faglia, M. Ferroni, A. Vomiero, and G. Sberveglieri, "Quasi-One Dimensional Metal Ooxide Semiconductors: Preparation, Characterization and Application as Chemical Sensors," *Prog. Mater. Sci.*, **54** [1] 1-67 (2009).
59. Z. U. Abideen, A. Katoch, J. H. Kim, Y. J. Kwon, H. W. Kim, and S. S. Kim, "Excellent Gas Detection of ZnO Nanofibers by Loading with Reduced Graphene Oxide Nanosheets," *Sens. Actuators, B,* **221** 1499-507 (2015).
60. E. S. Medeiros, G. M. Glenn, A. P. Klamczynski, W. J. Orts, and L. H. Cmattoso, "Solution Blow Spinning: A New Method to Produce Micro- and Nanofibers From Polymer Solutions," *J. Appl. Poly. Sci.*, **113** [4] 2322-30 (2009).
61. N. Li and C. R. Martin, "A High-Rate, High-Capacity, Nanostructured Sn-Based Anode Prepared Using Sol-Gel Template Synthesis," *J. Electrochem. Soc.*, **148** A164-70 (2001).
62. X. Zhang and Y. Lu, "Centrifugal Spinning: An Alternative Approach to Fabricate Nanofibers at High Speed and Low Cost," *Polym. Rev.,* **54** [4] 677-701 (2014).
63. K. L. Niece, J. D. Hartgerink, J. J. J. M. Donners, and S. I. Stupp, "Self-Assembly Combining Two Bioactive Peptide-Amphiphile Molecules into Nanofibers by Electrostatic Attraction," *J. Am. Chem. Soc.,* **125** [24] 7146-7 (2003).
64. S. Wang, F. Hu, J. Li, S. Zhang, M. Shen, M. Huang, and X. Shi, "Design of Electrospun Nanofibrous Mats for Osteogenic Differentiation of Mesenchymal Stem Cells," *Nanomedicine*, in press.
65. D. Li and Y. Xia, "Electrospinning of Nanofibers: Reinventing the Wheel?," *Adv. Mater.,* **16** [14] 1151-70 (2004).
66. R. Ramakrishnan, S. Subramanian, J. Rajan, and S. Ramakrishna, "Nanostructured Ceramics by Electrospinning," *J. Appl. Phys.,* **102** [11] 111101 (2007).
67. D. H. Reneker and A. L. Yarin, "Electrospinning Jets and Polymer Nanofibers," *Polymer*, **49** [10] 2387-425 (2008).
68. J. Doshi and D. H. Reneker, "Electrospinning Process and Applications of Electrospun Fibers," *J. Electrost.,* **35** [2] 151-60 (1995).
69. J. P. F. Lagerwall, J. T. Mccann, E. Formo, G. Scalia, and Y. Xia, "Coaxial Electrospinning of Microfibres with Liquid Crystal in the Core," *Chem. Commun.,* [42] 5420-2 (2008).
70. P. D. Dalton, D. Grafahrend, K. Klinkhammer, D. Klee, and M. Möller, "Electrospinning of Polymer Melts: Phenomenological Observations," *Polymer*, **48** [23] 6823-33 (2007).
71. A. V. Bazilevsky, A. L. Yarin, and C. M. Megaridis, "Co-Electrospinning of Core-Shell Fibers Using a Single-Nozzle Technique," *Langmuir*, **23** [5] 2311-4 (2007).
72. A. L. Yarin, E. Zussman, J. H. Wendorff, and A. Greiner, "Material Encapsulation and Transport in Core-Shell Micro/Nanofibers, Polymer and Carbon Nanotubes and Micro/Nanochannels," *J. Mater. Chem.,* **17** [25] 2585-99 (2007).
73. C. J. Luo, S. D. Stoyanov, E. Stride, E. Pelan, and M. Edirisinghe, "Electrospinning Versus Fibre Production Methods: From Specifics to Technological Convergence," *Chem. Soc. Rev.,* **41** [13] 4708-35 (2012).
74. S. Chigome and N. Torto, "A Review of Opportunities for Electrospun Nanofibers in Analytical Chemistry," *Anal. Chim. Acta,* **706** [1] 25-36 (2011).
75. S. Thenmozhi, N. Dharmaraj, K. Kadirvelu, and H. Y. Kim, "Electrospun Nanofibers: New Generation Materials for Advanced Applications," *Mater. Sci. Eng., B,* **217** 36-48 (2017).
76. A. Greiner and J. H. Wendorff, "Electrospinning: A Fascinating Method for the Preparation of Ultrathin Fibers," *Angew. Chem., Int. Ed.,* **46** [30] 5670-703 (2007).
77. D. Li, J. T. Mccann, Y. Xia, and M. Marquez, "Electrospinning: A Simple and Versatile Technique for Producing Ceramic Nanofibers and Nanotubes," *J. Am. Ceram. Soc.*, **89** [6] 1861-9 (2006).
78. B. Sun, Y. Z. Long, Z. J. Chen, S. L. Liu, H. D. Zhang, J. C. Zhang, and W. P. Han, "Recent Advances in Flexible and Stretchable Electronic Devices via Electrospinning," *J. Mater. Chem. C*, **2** [7] 1209-19 (2014).
79. W. E. Teo and S. Ramakrishna, "A Review on Electrospinning Design and Nanofibre Assemblies," *Nanotechnology*, **17** [14] R89 (2006).
80. R. Kessick, J. Fenn, and G. Tepper, "The Use of AC Potentials in Electrospraying and Electrospinning Processes," *Polymer*, **45** [9] 2981-4 (2004).
81. Z. M. Huang, Y. Z. Zhang, M. Kotaki, and S. Ramakrishna, "A Review on Polymer Nanofibers by Electrospinning and Their Applications in Nanocomposites," *Compos. Sci. Technol.,* **63** [15] 2223-53 (2003).
82. A. L. Yarin, S. Koombhongse, and D. H. Reneker, "Taylor Cone and Jetting From Liquid Droplets in Electrospinning of Nanofibers," *J. Appl. Phys.,* **90** [9] 4836-46 (2001).
83. M. M. Hohman, M. Shin, G. Rutledge, and M. P. Brenner, "Electrospinning and Electrically Forced Jets. I. Stability Theory," *Phys. Fluids,* **13** [8] 2201-20 (2001).
84. X. Lu, C. Wang, and Y. Wei, "One-Dimensional Composite Nanomaterials: Synthesis by Electrospinning and Their Applications," *Small*, **5** [21] 2349-70 (2009).
85. A. Katoch, S. W. Choi, and S. S. Kim, "Nanograins in Electrospun Oxide Nanofibers," *Met. Mater. Int.,* **21** [2] 213-21 (2015).
86. A. Katoch, G. J. Sun, S. W. Choi, J. H. Byun, and S. S. Kim, "Competitive Influence of Grain Size and Crystallinity on Gas Sensing Performances of ZnO Nanofibers," *Sens. Actuators, B,* **185** 411-6 (2013).
87. A. Katoch, J. H. Kim, and S. S. Kim, "Significance of the Nanograin Size on the H_2S-Sensing Ability of CuO-SnO_2 Composite Nanofibers," *J. Sens.*, **2015** 1-7 (2015).
88. A. Katoch, S. W. Choi, G. J. Sun, H. W. Kim, and S. S. Kim, "Mechanism and Prominent Enhancement of Sensing Ability to Reducing Gases in p/n Core-Shell Nanofiber," *Nanotechnology,* **25** 175501-8 (2014).

89. J. Y. Park, S. W. Choi, J. W. Lee, C. Lee, and S. S. Kim, "Synthesis and Gas Sensing Properties of TiO_2-ZnO Core-Shell Nanofibers," *J. Am. Ceram. Soc.,* **92** [11] 2551-54 (2009).
90. A. Katoch, J. H. Kim, and S. S. Kim, "TiO_2/ZnO Inner/Outer Double-Layer Hollow Fibers for Improved Detection of Reducing Gases," *ACS Appl. Mater. Interfaces,* **6** [23] 21494-9 (2014).
91. Z. L. Wang, Z. Li, J. Sun, H. Zhang, W. Wang, W. Zheng, and C. Wang, "Improved Hydrogen Monitoring Properties Based on p-NiO/n-SnO_2 Heterojunction Composite Nanofibers," *J. Phys. Chem. C*, **114** [13] 6100-5 (2010).
92. X. J. Zhang and G. J. Qiao, "High Performance Ethanol Sensing Films Fabricated From ZnO and In_2O_3 Nanofibers with a Double-Layer Structure," *Appl. Surf. Sci.,* **258** [17] 6643-47 (2012).
93. C. S. Lee, I. D. Kim, and J. H. Lee, "Selective and Sensitive Detection of Trimethylamine Using ZnO-In_2O_3 Composite Nanofibers," *Sens. Actuators, B,* **181** 463-70 (2013).
94. C. Feng, X. Li, J. Ma, Y. Sun, C. Wang, P. Sun, J. Zheng, and G. Lu, "Facile Synthesis and Gas Sensing Properties of In_2O_3-WO_3 Heterojunction Nanofibers," *Sens. Actuators, B,* **209** 622-29 (2015).
95. C. Feng, C. Wang, P. Cheng, X. Li, B. Wang, Y. Guan, J. Ma, H. Zhang, Y. Sun, P. Sun, J. Zheng, and G. Lu, "Facile Synthesis and Gas Sensing Properties of La_2O_3-WO_3 Nanofibers," *Sens. Actuators, B,* **221** 434-42 (2015).
96. W. Qin, L. Xu, J. Song, R. Xing, and H. Song, "Highly Enhanced Gas Sensing Properties of Porous SnO_2-CeO_2 Composite Nanofibers Prepared by Electrospinning," *Sens. Actuators, B,* **185** 231-37 (2013).
97. H. Du, J. Wang, M. Su, P. Yao, Y. Zheng, and N. Yu, "Formaldehyde Gas Sensor Based on SnO_2/In_2O_3 Hetero-Nanofibers by a Modified Double Jets Electrospinning Process," *Sens. Actuators, B,* **166** 746-52 (2012).
98. C. Feng, W. Li, C. Li, L. Zhu, H. Zhang, Y. Z. Zhang, S. Ruan, W. Chen, and L. Yu, "Highly Efficient Rapid Ethanol Sensing Based on In_2-xNixO_3 Nanofibers," *Sens. Actuators, B,* **166** 83-8 (2012).
99. Z. C. Sun, E. Zussman, A. L. Yarin, J. H. Wendorff, and A. Greiner, "Compound Core-Shell Polymer Nanofibers by Co-Electrospinning," *Adv. Mater.,* **15** [22] 1929-32 (2003).
100. M. F. Elahi, W. Lu, G. Guoping, and F. Khan, "Core-Shell Fibers for Biomedical Applications-A Review," *J. Bioeng. Biomed. Sci.,* **3** [1] 1-14 (2013).
101. R. Khajavi and M. Abbasipour, "Electrospinning as a Versatile Method for Fabricating Coreshell, Hollow and Porous Nanofibers," *Sci. Iran.,* **19** [6] 2029-34 (2012).
102. J. H. Wendorff, S. Agarwal, and A. Greiner, Electrospinning Materials, Processing, and Applications; pp. 155-58, Wiley-VCH Verlag & Co. KGaA, Singapore, 2012.
103. V. Merkle, L. Zeng, W. Teng, M. Slepian, and X. Wu, "Gelatin Shells Strengthen Polyvinyl Alcohol Core/Shell Nanofibers," *Polymer*, **54** 6003-7 (2013).
104. G. Korotcenkov, "Metal Oxides for Solid-State Gas Sensors: What Determines Our Choice?," *J. Mater. Sci. Eng. B,* **139** [1] 1-23 (2007).
105. G. Korotcenkov, "Gas Response Control through Structural and Chemical Modification of Metal Oxide Films: State of the Art and Approaches," *Sens. Actuators, B,* **107** [1] 209-32 (2005).
106. N. Barsan and U. Weimar, "Conduction Model of Metal Oxide Gas Sensors," *J. Electroceram.,* **7** [3] 143-67 (2001).
107. C. O. Park and S. A. Akbar, "Ceramics for Chemical Sensing," *J. Mater. Sci.,* **38** [23] 4611-37 (2003).
108. A. Rothschild and K. Yigal, "The Effect of Grain Size on the Sensitivity of Nanocrystalline Metal-Oxide Gas Sensors," *J. Appl. Phys.,* **95** [11] 6374-80 (2004).
109. H. Ogawa, M. Nishikawa, and A. Abe, "Hall Measurement Studies and an Electrical Conduction Model of Tin Oxide Ultrafine Particle Films," *J. Appl. Phys.,* **53** [6] 4448-55 (1982).
110. M. Hübner, C. E. Simion, A. Tomescu-Stănoiu, S. Pokhrel, N. Bârsan, and U. Weimar, "Influence of Humidity on CO Sensing with p-Type CuO Thick Film Gas Sensors," *Sens. Actuators, B,* **153** [2] 347-53 (2011).
111. W. Wang, Z. Li, W. Zheng, H. Huang, C. Wang, and J. Sun, "Cr_2O_3-Sensitized ZnO Electrospun Nanofibers Based Ethanol Detectors," *Sens. Actuators, B,* **143** [2] 754-58 (2010).
112. F. L. Meng, Z. Guo, and X. J. Huang, "Graphene-Based Hybrids for Chemiresistive Gas Sensors," *TrAC, Trends Anal. Chem.,* **68** 37-47 (2015).
113. F. Schedin, Ga. K. Eim, S. V. Morozov, E. W. Hill, P. Blake, M. I. Katsnelson, and K. S. Novoselov, "Detection of Individual Gas Molecules Adsorbed on Graphene," *Nat. Mater.,* **6** [9] 652-55 (2007).
114. W. Yuan and G. Shi, "Graphene-Based Gas Sensors," *J. Mater. Chem. A,* **1** [35] 10078-91 (2013).
115. F. Yavari and N. Koratkar, "Graphene-Based Chemical Sensors," *J. Phys. Chem. Lett.,* **3** [13] 1746-53 (2012).
116. S. Basu and P. Bhattacharyya, "Recent Developments on Graphene and Graphene Oxide Based Solid State Gas Sensors," *Sens. Actuators, B,* **173** 1-21 (2012).
117. J. H. Lee, A. Katoch, S. W. Choi, J. H. Kim, H. W. Kim, and S. S. Kim, "Extraordinary Improvement of Gas-Sensing Performances in SnO_2 Nanofibers Due to Creation of Local p-n Heterojunctions by Loading Reduced Graphene Oxide Nanosheets," *ACS Appl. Mater. Interfaces,* **7** 3101-9 (2015).
118. Z. U. Abideen, H. W. Kim, and S. S. Kim, "An Ultra-Sensitive Hydrogen Gas Sensor Using Reduced Graphene Oxide-Loaded ZnO Nanofibers," *Chem. Commun.*, **51** 15418-21 (2015).
119. D. Wang, M. Zhang, Z. Chen, H. Li, A. Chen, X. Wang, and J. Yang, "Enhanced Formaldehyde Sensing Properties of Hollow SnO_2 Nanofibers by Graphene Oxide. *Sens. Actuators, B,* **250** 533-42 (2017).
120. W. Zeng, T. Liu, and Z. L. Wang, "Sensitivity Improvement of TiO_2-Doped SnO_2 to Volatile Organic Compounds," *Phys. E,* **43** [2] 633-8 (2010).
121. S. Ju, S. Kim, S. Mohammadi, D. B. Janes, Y. G. Ha, and A. Facchetti, "Interface Studies of ZnO Nanowire Transistors Using Low-Frequency Noise and Temperature-Dependent I-V Measurements," *Appl. Phys. Lett.,* **92** [2] 022104 (2008).
122. C. A. Pan and T. P. Ma, "Work Function of In_2O_3 Film as Determined From Internal Photoemission," *Appl. Phys. Lett.,* **37** [8] 714-16 (1980).

123. P. Feng, Q. Wan, and T. H. Wang, "Contact-Controlled Sensing Properties of Flowerlike ZnO Nanostructures," *Appl. Phys. Lett.,* **87** [21] 213111 (2005).
124. P. Feng, X. Y. Xue, Y. G. Liu, and T. H. Wang, "Highly Sensitive Ethanol Sensors Based on {100}-Bounded In_2O_3 Nanocrystals Due to Face Contact," *Appl. Phys. Lett.,* **89** [24] 243514 (2006).
125. A. Kolmakov and M. Moskovits, "Chemical Sensing and Catalysis by One-Dimensional Metal-Oxide Nanostructures," *Annu. Rev. Mater. Res.,* **34** 151-80 (2004).
126. J. Gao, L. Wang, K. Kan, S. Xu, L. Jing, Ls. Iu, P. Shen, L. Li, and K. Shi, "One-Step Synthesis of Mesoporous Al_2O_3-In_2O_3 Nanofibres with Remarkable Gas-Sensing Performance to NOx at Room Temperature," *J. Mater. Chem. A,* **2** [4] 949-56 (2014).
127. W. Li, S. Ma, Y. Li, G. Yang, Y. Mao, J. Luo, D. Gengzang, X. Xu, and S. Yan, "Enhanced Ethanol Sensing Performance of Hollow ZnO-SnO_2 Core-Shell Nanofibers. *Sens. Actuators, B,* **211** 392-402 (2015).
128. H. Du, J. Wang, Y. Sun, P. Yao, X. Li, and N. Yu, "Investigation of Gas Sensing Properties of SnO_2/In_2O_3 Composite Hetero-Nanofibers Treated by Oxygen Plasma," *Sens. Actuators, B,* **206** 753-63 (2015).
129. X. Yang, V. Salles, Y. V. Kaneti, M. Liu, M. Maillard, C. Journet, X. Jiang, and A. Brioude, "Fabrication of Highly Sensitive Gas Sensor Based on Au Functionalized WO_3 Composite Nanofibers by Electrospinning," *Sens. Actuators, B,* **220** 1112-9 (2015).
130. Y. Lin, W. Wei, Y. Li, F. Li, J. Zhou, D. Sun, Y. Chen, and S. Ruan, "Preparation of Pd Nanoparticle-Decorated Hollow SnO_2 Nanofibers and Their Enhanced Formaldehyde Sensing Properties," *J. Alloys Compd.,* **651** 690-98 (2015).
131. X. Xu, Y. Chen, G. Zhang, S. Ma, Y. Lu, H. Bian, and Q. Chen, "Highly Sensitive VOCs-Acetone Sensor Based on Ag-Decorated SnO_2 Hollow Nanofibers," *J. Alloys Compd.,* **703** 572-79 (2017).
132. N. Kim, H. Choi, J. Seon, D. Yang, J. Bae, J. Park, and I. D. Kim, "Highly Sensitive and Selective Hydrogen Sulfide and Toluene Sensors Using Pd Functionalized WO_3 Nanofibers for Potential Diagnosis of Halitosis and Lung Cancer," *Sens. Actuators, B,* **193** 574-81 (2014).
133. A. Katoch, S. W. Choi, J. H. Kim, J. H. Lee, J. S. Lee, and S. S. Kim, "Importance of the Nanograin Size on the H_2S-Sensing Properties of ZnO-CuO Composite Nanofibers," *Sens. Actuators, B,* **214** 111-16 (2015).
134. H. Wu, K. Kan, L. Wang, G. Zhang, Y. Yang, and H. Li, "Electrospinning of Mesoporous p-Type In_2O_3/TiO_2 Composite Nanofibers for Enhancing NOx Gas Sensing Properties at Room Temperature," *CrystEngComm,* **16** [38] 9116-24 (2014).
135. J. Cao, Z. Y. Wang, R. Wang, S. Liu, T. Fei, and L. J. Wang, "Synthesis of Core-Shell α-Fe_2O_3@NiO Nanofibers with Hollow Structures and Their Enhanced HCHO Sensing Properties," *J. Mater. Chem. A*, **3** 5635-41 (2015).
136. Y. Liu, X. Sun, B. Li, and Y. Lei, "Tunable p-n Transition Behaviour of a p-$La_{0.67}Sr_{0.33}MnO_3$/n-CeO_2 Nanofibers Heterojunction for the Development of Selective High Temperature Propane Ssensors," *J. Mater. Chem. A*, **2** 11651-59 (2014).
137. C. Li, C. H. Feng, F. D. Qu, J. Liu, L. H. Zhu, and Y. Lin, "Electrospun Nanofibers of p-Type NiO/n-Type ZnO Heterojunction with Different NiO Content and Its Influence on Trimethylamine Sensing Properties," *Sens. Actuators, B,* **207** 90-6 (2015).
138. L. Liu, Y. Zhang, G. G. Wang, S. C. Li, L. Y. Wang, and Y. Han, "High Toluene Sensing Pproperties of NiO-SnO_2 Composite Nanofiber Sensors Operating at 330 Degrees C," *Sens. Actuators, B,* **160** 448-54 (2011).
139. X. Liang, T. H. Kim, J. W. Yoon, C. H. Kwak, and J. H. Lee, "Ultrasensitive and Ultraselective Detection of H_2S Using Electrospun CuO-Loaded In_2O_3 Nanofiber Sensors Assisted by Pulse Hheating," *Sens. Actuators, B,* **209** 934-42 (2015).
140. Y. Zheng, J. Wang, and P. Yao, "Formaldehyde Sensing Properties of Electrospun NiO-Doped SnO_2 Nanofibers," *Sens. Actuators, B,* **156** 723-30 (2011).
141. A. Katoch, S. W. Choi, G. J. Sun, and S. S. Kim, "An Approach to Detecting a Reducing Gas by Radial Modulation of Electron-Depleted Shells in Core-Shell Nanofibers," *J. Mater. Chem. A*, **1** 13588-96 (2013).
142. A. Yang, X. Tao, R. Wang, S. Lee, and C. Surya, "Room Temperature Gas Sensing Properties of SnO_2/Multiwall-Carbon-Nanotube Composite Nanofibers," *Appl. Phys. Lett.*, **91** 133110-13 (2007).
143. Y. H. Li, J. Gong, G. H. He, and Y. L. Deng, "Fabrication of Polyaniline/Titanium Dioxide Composite Nnanofibers for Gas Sensing Application," *Mater. Chem. Phys.,* **129** 477-82 (2011).
144. W. Tang, J. Wang, P. J. Yao, and X. G. Li, "Hollow Hierarchical SnO_2-ZnO Composite Nanofibers with Hheterostructure Based on Electrospinning Method for Detecting Methanol," *Sens. Actuators, B,* **192** 543-49 (2014).
145. T. A. Ho, T. S. Jun, and Y. S. Kim, "Material and NH_3-Sensing Properties of Polypyrrole-Coated Tungsten Oxide Nanofibers," *Sens. Actuators, B,* **185** 523-29 (2013).
146. S. Yan and Q. S. Wu, "Micropored Sn-SnO_2/Carbon Heterostructure Nanofibers and Their Highly Sensitive and Selective C_2H_5OH Gas Sensing Performance," *Sens. Actuators, B,* **205** 329-37 (2014).
147. J. A. Deng, B. Yu, Z. Lou, L. L. Wang, R. Wang, and T. Zhang, "Facile Synthesis and Enhanced Ethanol Sensing Properties of the Brush-Like ZnO-TiO_2 Heterojunctions Nanofibers," *Sens. Actuators, B*, **184** 21-6 (2013).
148. Q. Qi, Y. C. Zou, M.-H. Fan, Y. P. Liu, S. Gao, and P. P. Wang, "Trimethylamine Sensors with Enhanced Anti-Humidity Ability Fabricated From $La_{0.7}Sr_{0.3}FeO_3$ Coated In_2O_3-SnO_2 Ccomposite Nanofibers," *Sens. Actuators, B,* **203** 111-17 (2014).
149. Q. Qi, P. P. Wang, J. Zhao, L. L. Feng, L. J. Zhou, and R. F. Xuan, "SnO_2 Nanoparticle-Coated In_2O_3 Nanofibers with Improved NH_3 Sensing Properties," *Sens. Actuators, B,* **194** 440-46 (2014).
150. B. B. Wang, X. X. Fu, F. Liu, S. L. Shi, J. P. Cheng, and X. B. Zhang, "Fabrication and Gas Sensing Pproperties of Hollow Core-Shell SnO_2/α-Fe_2O_3 Heterogeneous Structures," *J. Alloys Compd.*, **587** 82-9 (2014).